Intrusion of summer Alaskan Coastal Water in the western Arctic Ocean from 1999 to 2019: insights into interannual trends and driving mechanism

Xinyuan Lv[1, 2] and Na Liu[1, 2*]

[1]Key Laboratory of Marine Science and Numerical Modeling, Ministry of Natural Resources, Qingdao, China.

[2]Qingdao National Laboratory for Marine Science and Technology, Qingdao, China.

Corresponding author: Na Liu (liun@fio.org.cn)

Key Points:

- Western Arctic Ocean
- Alaskan Coastal Water (ACW)
- Interannual trends

Abstract

This work is a study of the interannual variability of Alaskan Coastal Water (ACW) supplied into the Arctic Ocean during the summer season. Based on hydrological data obtained during ten Chinese National Arctic Research Expeditions conducted in the summer from 1999 to 2019, the expansion of area, volume, thickness, and heat content of ACW in the southern Chukchi Sea and northern Bering Sea have been calculated for the first time, demonstrating the presence of substantial interannual variability. From 1999 to 2019, in general, each of the fundamental parameters showed two stages, namely 1999-2008 and 2010-2019, with the latter being at a higher value than the former. We repeatedly surveyed meridional hydrographic/velocity sections in the vicinity of the Bering Strait to verify that the changes in the water mass flowing into the strait are the main factors affecting water parameters in both the northern Bering Strait and the southern Chukchi Sea.

Plain Language Summary

The Bering Strait is the sole connection between the Pacific and Arctic Oceans. Alaskan Coastal Water (ACW) is one of the main ocean currents that merge into the Arctic Ocean through the Bering Strait from the Pacific Ocean. Its basic characteristics such as temperature and salinity directly affect the freshwater content and heat budget of the Arctic. Based on the Chinese National Arctic Research Expeditions, it is found that near the Chukchi Sea, the characteristics of the interannual variation of ACW from 2010 to 2019 are significantly different from that from 1999 to 2008. Further research shows that this is closely related to the flow into the Bering Strait.

1 Introduction

The seasonally ice-covered Bering and Chukchi Sea shelves are among the largest continental shelves in the world (Grebmeier et al., 2006). The Bering Strait Complex (Anadyr Strait, Shpanberg Strait, and Bering Strait) in the northern Bering Sea and southern Chukchi Sea is the sole connection between the Pacific and Arctic Oceans. The flow through the Bering Strait is the only oceanic input from the Pacific into the Arctic Ocean (AO) (Woodgate, 2018).

Pacific water inflow through this complex is an important source of heat, freshwater, nutrients and Pacific fauna into the AO (Woodgate & Aagaard, 2005; Woodgate et al., 2005; Grebmeier et al., 2006), specifically in the lower layers of the AO, including in the layer of summer Pacific water. Pacific waters, supplied through the Bering Strait, form one third of the incoming water volume responsible for the AO fresh water balance, and are a powerful heat source, which can influence the thickness and distribution of the sea ice cover (Woodgate & Aagaard, 2005; Makhotina & Dmitrenkob, 2011). In summertime, the warm water input melts pack ice (Weingartner et al., 2005) accounting for the greatest interannual variability in Arctic freshwater input (Johanna et al., 2017). Pacific water also contributes to the stratification of the water column over large areas of the western Arctic, helping to maintain the upper halocline (Anderson et al., 2013; Johanna et al., 2017).

In order to reach the central Arctic Ocean, Pacific water must first cross the wide and shallow Chukchi Sea (Johanna et al., 2017). There are three main flow pathways by which this occurs, dictated largely by the topography of the shelf (Weingartner et al., 2005): the Alaskan Coastal Water (ACW) on the east, the Bering Shelf Water (BSW) in the central area, and the Anadyr Water (AW) on the west (Grebmeier et al., 2006; Yamashita et al., 2019).

In this paper, we mainly study the warmer, less saline, low-nutrient ACW, also known as the Eastern Chukchi Summer Water (ECSW), which flows northward along the coast of Alaska toward Barrow Canyon and is referred to as the Alaskan Coastal Current (ACC) in the warm months of the year (Lin et al., 2019). Alaskan coastal water originates along the coast over the inner shelf in the eastern Bering Sea; it develops annually from the input of river water and melting ice from western Alaskan rivers and its temperature increases rapidly through the spring and summer from about 0 to 10 C° (Eisner et al., 2013). This current is believed to provide ~0.1 Sv of flow, ~1/3 of the heat and 1/4 of the freshwater fluxes through the strait (Woodgate & Aagaard, 2005; Woodgate, 2018).

The increase in annual mean transport is reflected in correspondingly significant increases in the annually integrated fluxes of heat and fresh water. In the present study, we estimate the interannual variability of the ACW in relation to area expansion, volume, thickness, and heat content. The analysis has been made for the first time based on summer data obtained from repeated sections set up in the southern Chukchi Sea and northern Bering Sea (66°N-75°N) in the 1999-2019 period. Additionally, in order to explain the characteristics of the interannual variation of ACW entering the Arctic Ocean, we analyzed the volume and heat fluxes from the zonal section of the southern Bering Strait (172°W-167°W).

2 Data and methods

2.1 Data

2.1.1 The conductivity-temperature-depth (CTD) Data

From 1999 to2019, ten repeated zonal hydrographic/velocity sections were set up in the vicinity of the southern Chukchi Sea and northern Bering Sea during ten Arctic research expeditions conducted by China. These cruises occurred in the summer, and even though the timing of each cruise varied among years, it can be considered quasi-synchronous. We labeled these transects as R and the bottom depth in the study area was 50 m. The latitude range of these sections was about 66°-75°N, while the longitude range was 170°-172°W. Additionally, several meridional transects were also set up during the expeditions at the south end of the Bering strait and across the northern Bering Sea shelf, and they were labelled either BS, NB or BN. The depth of every station was also less than 50 m, the latitude range of the sections was approximately 64.2°-64.6°N, and the longitude range was 167°-171.7°W (Wang et al., 2020).

These two repeated sections both have a distance of less than 1° between stations. Exact locations of the stations are shown in Figure 1.

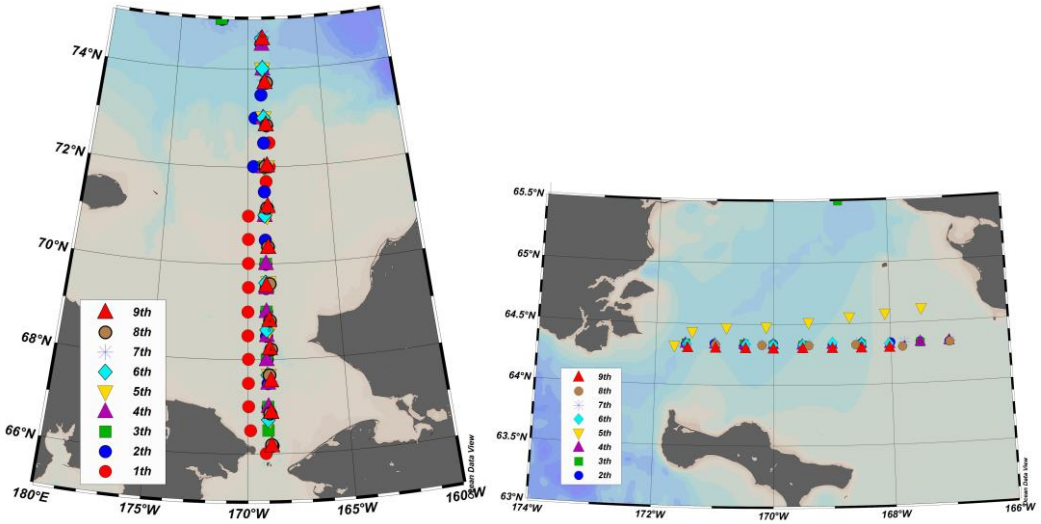

Figure 1. Distribution of R sections (left) and BS/NB/BN sections (right) collected by the first nine Chinese National Arctic Research Expeditions.

2.1.2 HYCOM Reanalysis Data

To analyze the volume and heat fluxes and to apply arithmetic corrections (see section 2.2), we used reanalysis data from the Hybrid Coordinate Ocean Model (HYCOM). This model includes daily in-situ temperature, sea water salinity, eastward and northward sea water velocity with a uniform 0.08 degree lat/lon grid between 80.48°S and 80.48°N interpolated to 40 standard z-levels. (Li et al., 2019)

2.1.3 Water mass identification

In the Chukchi Sea, water masses that originate from the Pacific Ocean in the summer are characterized by temperature (T) and salinity (S) (Nishino et al., 2016). According to Danielson et al., the ACW temperature is not significantly different in the two areas of the southern Chukchi Sea and northern Bering Sea, and the ACW salinity in the northern Bering Sea is within a smaller value. During the midsummer period of 2012 and 2013, the salinity range was roughly 20-32 psu (Danielson et al., 2017). The combined T/S diagram from data collected during the research expeditions illustrates the typical summer conditions in the southern Chukchi Sea and northern Bering Sea (Figure 2) (Gong & Pickart, 2015). To analyze the CTD data, we used ACW definitions presented in previous studies and that are consistent with our data. However, the precise definition of each water mass should not be considered invariable because water properties can change considerably from one year to the next, and, to some extent, from season to season (Gong & Pickart, 2015). In this paper, ACW is characterized by potential temperatures ≥5C° and by salinities ≤31.8 psu (Grebmeier et al., 2006; Gong & Pickart, 2015; Nishino et al., 2016; Danielson et al., 2017).

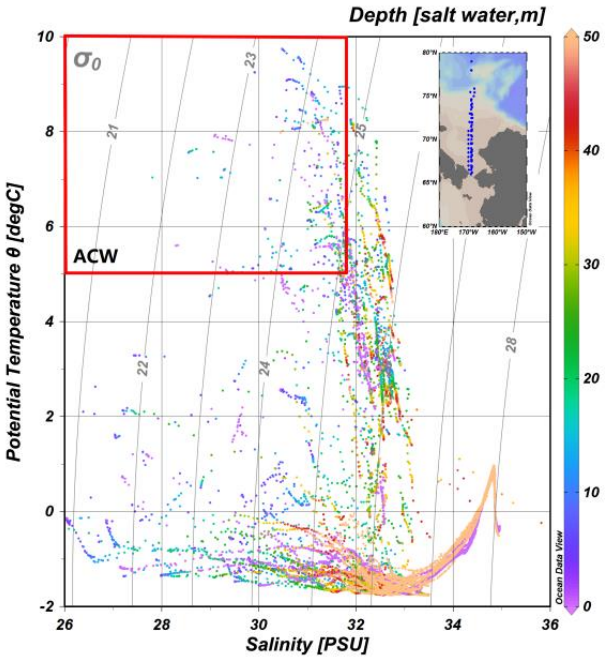

Figure 2. Temperature-Salinity plot of water masses in the southern Chukchi Sea and northern Bering Sea (The area in the red box is the ACW water mass defined in this paper, with T≥5℃and S≤31.8psu)

2.2 Methods

2.2.1 Calibration of CTD data

It was anticipated that, due to the large difference in the time of CTD deployment during each expedition, calculations of heat flux, volume flux and heat content from datasets would be inaccurate. In order to solve this problem, CTD data were calibrated according to the HYCOM reanalysis data, and were corrected for the time difference. As far as the R sections are concerned, the data from each expedition were all calibrated to August 31 (Table 1), while the data from the BS/NB/BN sections were all calibrated to July 26 (Table 2).

Firstly, the grid point data closest to the latitude and longitude of each CTD station were identified in the HYCOM reanalysis data, then the closest depth was located. The average depth near the Bering Strait (that is, near the R and BS sections) was 55m, and the available levels in the HYCOM reanalysis data were only 0, 2, 4, 6, 8, 10, 12, 15, 20, 25, 30, 35, 40, 45 and 50m. Finally, the corresponding two days in the HYCOM reanalysis data were subtracted to calculate the difference, and this difference was used to correct the CTD data.

Table 1. Calibration date for each expedition in the R sections

Expedition(time)	Original date	Calibrate date
1th(1999)	August 3	August 31
2th(2003)	July 30	August 31
3th(2008)	August 1	August 31

4th(2010)	July 20	August 31
5th(2012)	September 8	August 31
6th(2014)	July 31	August 31
7th(2016)	September 4	August 31
8th(2017)	Num1: September 10	August 31
	Num1-12: September 22	
9th(2018)	September 7	August 31

Table 2. Calibration date for each expedition in the BS/NB/BN sections

Expedition(time)	Original date	Calibrate date
2th(2003)	July 28	July 26
4th(2010)	July 19	July 26
5th(2012)	July 17	July 26
7th(2016)	September 8	July 26
8th(2017)	September 24	July 26
9th(2018)	September 8	July 26
10^{th}(2019)	August 29	July 26

2.2.2 Ocean Heat Content (OHC)

In this study, the heat content for each station in the R sections was defined as the integrated ocean heat content from a depth of 50 m to sea surface, and it was calculated using the following formula:

$$\mathrm{OHC} = \int_{-50}^{0} 4\pi^2 R^2 \rho(T,S) C_p T \cos\phi / 259200 dh$$

where R is the radius of the earth, T is the in situ temperature, S is sea water salinity, ρ(T, S) is the density of seawater, varying with temperature (T) and salinity (S) at depth h, C_p is the specific heat of seawater, ϕ is the latitude of each station (Ishii & Kimoto, 2009; Wang et al., 2013).

In addition, CTD temperature and salinity data were interpolated before calculating the heat content, with 0-50 m per meter and 66°N-73°N every 0.1°.

2.2.3 Thickness, area and volume

The ACW depth at each CTD site was calculated individually at each station based on the corrected and interpolated data. The average ACW depth at each site was considered as the final thickness value. Because the longitude range between any two stations in the entire R section for each cruise was less than 1° (and data reliability of stations less than 1° apart is very high after interpolation), the longitude range was

uniformly set as 1° when calculating the ACW distribution area. The longitude distance of 1° on latitude A was calculated based on the formula, 111*cos(A). Since the interval length of a 1° latitude is the same all over the world, the latitude range was converted into km based on the 111km/1° ratio. Because the Earth is not a perfect sphere, the area was calculated by averaging the latitude range at the upper and lower latitudes as "long" and taking the latitude range as "wide". Volume was obtained by multiplying thickness by area, both derived from of the above calculations.

2.2.4 Flux of water masses

We used temperature and salinity CTD data (after calibration) and velocity reanalysis data from the HYCOM to examine the volume flux (V) and heat flux (H) flowing over the northern Bering Sea shelf from 1999 to 2018. Since the number of stations and the longitudinal ranges were different each year, we interpolated the data before calculating the fluxes, with 0-50 m per meter and 172°W-167°W every 0.5°. The volume and heat fluxes (with northward positive direction) (Wang et al., 2020) were calculated using the following equations:

$$V = \sum A_i \cdot v_{ni}$$

$$H = \sum C_p \cdot A_i \cdot \rho_i \cdot v_{ni} \cdot T_i$$

where A_i is the area of i grid, v_{ni} is the meridional component of the i grid current in n station, C_p is the constant pressure specific heat of sea water, the measuring unit is $J \cdot kg^{-1} \cdot ℃^{-1}$, ρ_i is the density of sea water and T_i is the temperature.

3 Results

The interannual variations in terms of distribution area, thickness, volume and heat content were divided into two distinct groups: one for years 1999 to 2008 presenting a low level, and the other for years 2010 to 2019, with a relatively high value.

Based on the obtained data on interannual variability, the largest distribution area of ACW in the southern Chukchi Sea and northern Bering Sea was observed in 2019 exceeding the value of 2017 (when the ACW volume was maximal) by 0.39×10^4 km^2 (Figure 3). The minimal values for area and volume were observed both in 1999 and 2008. In 2008 volume was slightly smaller than in 1999, while the distribution area was slightly smaller in 1999 than in 2008. The overall variation in volume and area was entirely consistent from 1999 to 2016, while the trend of interannual change from 2016 to 2019 was highly inconsistent. Based on the data for interannual change in thickness observed in ACW from 2016 to 2019, it is possible to conclude that this variation in thickness determined the opposite trend variation seen for volume and area during this time period.

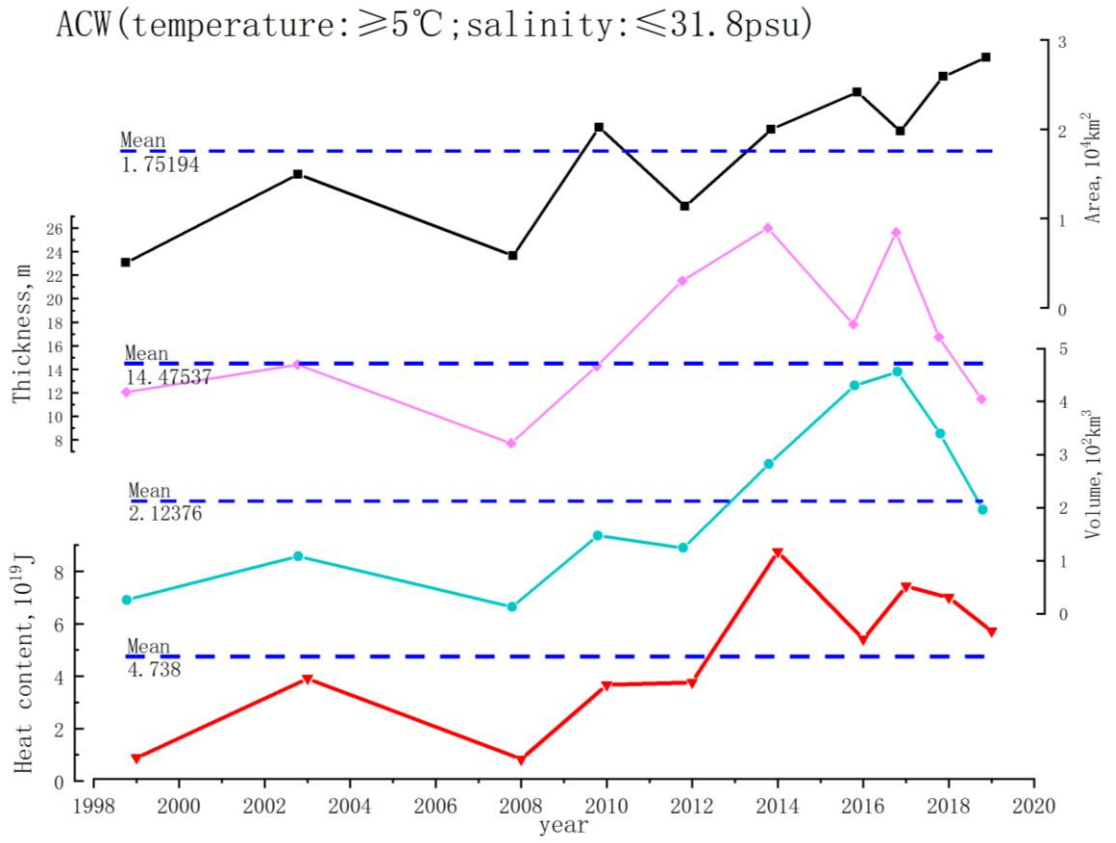

Figure 3. Interannual variability of distribution area (black), thickness (pink), volume (blue), and heat content (red) of ACW in the southern Chukchi Sea and northern Bering Sea.

Data reveal that the average heat content of ACW in the southern Chukchi Sea and northern Bering Sea in the 1999-2019 period was 4.74×10^{19}J. It is worth noting that, although the overall change in heat content from 1999 to 2008 remained at a relatively low level, the heat content in 2003 increased significantly. Consistent with the ACW area and volume, the ACW heat content in 1999 and 2008 was remarkably below the climatological data recorded between 1999 and 2020 (Liu et al., 2012). In general, the time sequence for ACW parameters from 2008 to 2014 shows a statistically significant positive trend (heat content is 1.98×10^{19} J/yr), and in 2014 the heat content reached the maximal value (8.75×10^{19} J). From 2014 to 2019, the values decreased though a slight increase was observed between 2016 and 2017. Compared with the rising trend seen in the 2008-2014 period, the 2014-2019 trend decreased slowly and remained overall above the climatic average.

The water properties of the Chukchi Sea are predominantly determined by the water mass entering through the Bering Strait (Woodgate et al., 2005; Woodgate, 2018). In order to analyze interannual variability (Figure 3), we have considered the peculiarities of volume and heat transport of ACW through the Bering Strait to the Chukchi Sea shelf. In this section, we used the CTD temperature and salinity data (after calibration) and velocity reanalysis data from the HYCOM to examine the volume flux (V) and heat flux (H) flowing over the northern Bering Sea shelf from 1999 to 2018.

The longitude range of the repeated hydrographic/velocity sections was 167°-171.7°W (that was for the BN section, NB section and BS section). Since no similar section was available for the southern Bering Strait area in 1999, we used the temperature and salinity data from the HYCOM reanalysis data to supplement the missing data.

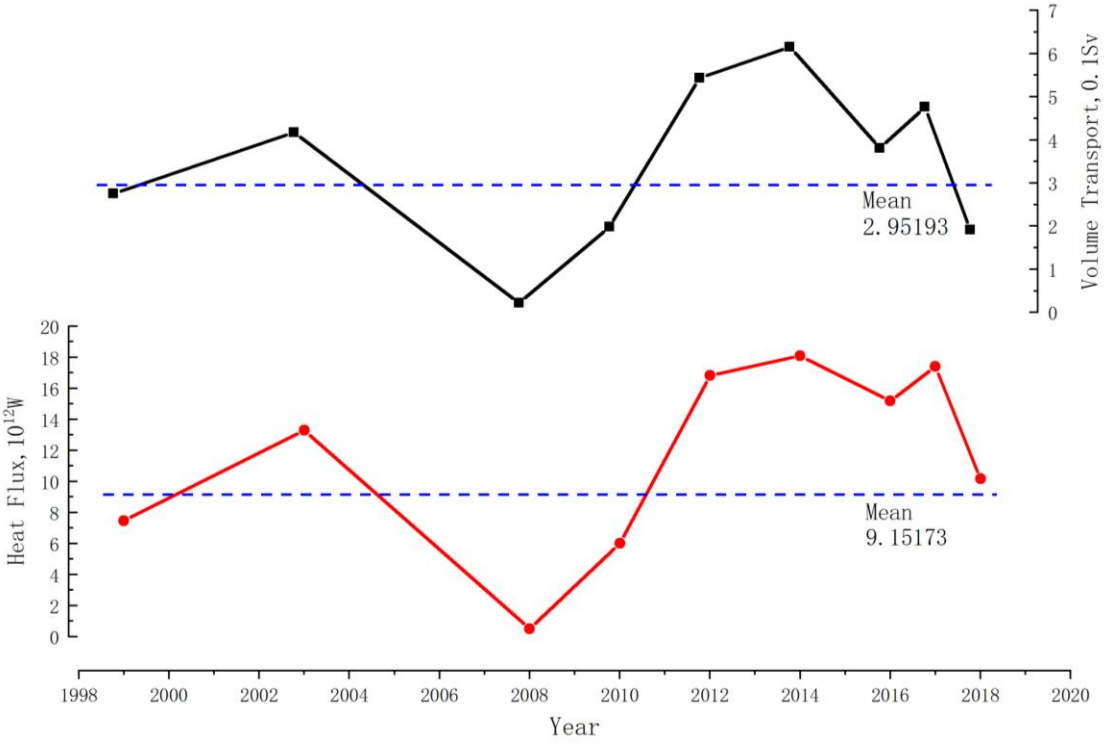

Figure 4. Interannual variability of volume transport (black) and heat flux (red) of ACW in the southern Bering Sea.

It was possible to conclude that the heat flow through the Bering Strait varies to a greater degree, compared to the water flow, and therefore, that it has a greater influence on ACW variability in the southern Chukchi Sea and northern Bering Sea. By comparing Figure 3 and Figure 4, it is visible that the general heat flux trend of the BS section in the southern Bering Strait is consistent with the general heat content trend of the R section in the southern Chukchi Sea and northern Bering Sea, although the range of change is slightly different in several time periods. For example, the rise in heat flux seen from 2010 to 2012 is significant than that seen from 2008 to 2010, while the increase in heat content seen from 2008 to 2010 is significant than that seen from 2010 to 2012. Overall, there is no doubt that the increase in heat flow through the Bering Strait leads to the interannual variability of the ACW in the southern Chukchi Sea and northern Bering Sea. Similarly, the change in volume transport through the Bering Strait can partially explain the interannual change in the ACW volume of the R sections. In addition, from 2008 to 2014 there was a continuous upward trend for volume transport through the Bering Strait, while there was a slight downward trend in the ACW volume between 2010 and 2012. Regardless of the volume or heat fluxes of the BS sections, the downward trend observed in the 2003-2008 period is more obvious than the upward trend seen between 1999 and 2003. Regardless of the ACW volume or

heat content at R sections, the downward trend observed from 2003 to 2008 is almost the same as the upward trend seen from 1999 to 2003.

4 Conclusions and Discussion

In summary, the expansion of area, volume, thickness, and heat content of ACW in the southern Chukchi Sea and northern Bering Sea have been calculated for the first time for the 1999–2019 period; the estimates demonstrate the presence of a significant interannual variability. All the analyzed parameters show that ACW in the southern Chukchi Sea and northern Bering Sea from 2010 to 2019 is significantly strengthened than in the 1999-2008 period. From 2017 to 2019, the ACW entering the Arctic has gradually become shallower and now shows a clear trend of northward expansion. In the 1999–2019 period, the inneranual variation of ACW characteristics was mainly determined by the heat and volume fluxes flowing through the Bering Strait. The significant interannual variability of distribution area, volume, and heat content observed in ACW in recent years influences the formation and variability of the thermohaline structure of the entire Arctic Ocean. We emphasize again that, although the volume and heat transport through the Bering Strait plays a major role in determining ACW parameters in the Arctic Ocean, wind force and input from rivers may also be important.

The results indicate that the peculiarities of ACW volume and heat transport through the Bering Strait to the Chukchi Sea shelf can explain the interannual variability of the characteristics of ACW, which flows into the Arctic Ocean during the summer season. However, other processes may also contribute to this variability. For example, wind strength and direction are important and direct factors influencing the velocity and flow of water masses; episodic wind-driven upwelling occurs along the northwestern Alaskan coast, displacing the easternmost branch of the Chukchi circulation seaward and weakening or reversing the flow that normally takes place along the coast (Woodgate et al., 2005). In addition, fresh water injection from Alaska's inland rivers also directly affects the inherent properties of ACW (Eisner et al., 2013).

Data Availability Statement

The CTD data in the southern Chukchi Sea and northern Bering Sea during ten Arctic research expeditions conducted by China are available at https://www.chinare.org.cn/data. The Hybrid Coordinate Ocean Model (HYCOM) data used to analyze the volume and heat fluxes and to apply arithmetic corrections were collected from https://www.hycom.org/dataserver/gofs-3pt0.

References

Anderson, L.G., Andersson, P.S., Bjork, G., Jones, E.P., Jutterstrom, S., & Wahlstrom, I. (2013). Source and formation of the upper halocline of the Arctic Ocean. *Journal of Geophysical Research: Oceans*, 118(1): 410–421. https://doi.org/10.1029/2012jc008291

Cai, X. J., Jiang, H., Wang, H., & Zuo, J. C. (2013). The relationship between tropical cyclone in the northwest Pacific and upper ocean heat content. *Acta Oceanologica Sinica (in Chinese)*, 35(3): 28–35. 蔡晓杰, 姜华, 王辉, 左军成. 西北太平洋热带气旋与上层海洋热含量的关系[J]. 海洋学报, 2013, 35(3): 28-35.

Danielson, S. L., Eisner, L., Carol, L., Mordy, C., Sousa, L., & Weingartner, T. J., (2017). A comparison between late summer 2012 and 2013 water masses, macronutrients, and phytoplankton standing crops in the northern Bering and Chukchi Seas. *Deep-Sea Research II*, 135: 7–26. http://dx.doi.org/10.1016/j.dsr2.2016.05.024

Eisner, L., Hillgruber, N., Martinson, E., & Maselko, J. (2013). Pelagic fish and zooplankton species assemblages in relation to water mass characteristics in the northern Bering and southeast Chukchi seas. *Polar Biology*, 36(1), 87–113. https://doi.org/10.1007/s00300-012-1241-0

Gong, D. L., Pickart, R. S. (2015). Summertime circulation in the eastern Chukchi Sea. *Deep-Sea Research II*, 118: 18–31. http://dx.doi.org/10.1016/j.dsr2.2015.02.006

Grebmeier, M. J., Cooper, L. W., Feder, H. M., & Sirenko B. K. (2006). Ecosystem dynamics of the Pacific-influenced Northern Bering and Chukchi Seas in the Amerasian Arctic. *Progress in Oceanography*, 71, 331–361. https://doi.org/10.1016/j.pocean.2006.10.001

Ishii, M., & Kimoto, M. (2009). Reevaluation of historical ocean heat content variations with time-varying XBT and MBT depth bias corrections. *Journal of Oceanography*, 65(3): 287–299. https://doi.org/10.1007/s10872-009-0027-7

Johanna, L., Pickart, R. S., Björk, G, & Moore G. W. K. (2017). On the nature and origin of water masses in Herald Canyon, Chukchi Sea: Synoptic surveys in summer 2004, 2008, and 2009, *Progress in Oceanography*, 159, 99–114. https://doi.org/10.1016/j.pocean.2017.09.005

Li, M., Pickart, R., S., Spall, M. A., Weingartner, T. J., Lin, P., Moore, G. W. K., & Qi, Y. Q. (2019). Circulation of the Chukchi Sea shelfbreak and slope from moored timeseries. *Progress in Oceanography*, 172: 14–33. https://doi.org/10.1016/j.pocean.2019.01.002

Lin, P., Pickart, R. S., McRaven, L. T., Arrigo, K. R., Bahr, F., Lowry, K. E., Stockwell, D. A., & Mordy, C. W. (2019). Water mass evolution and circulation of the northeastern Chukchi Sea in summer: Implications for nutrient distributions. *Journal of Geophysical Research: Oceans*, 124: 4416–4432. https://doi.org/10.1029/2019JC015185

Liu, N., Liu, J. P., Zhang, Z. H., Chen, H. X, & Mirong, S. (2012). Short Communication Is extreme Arctic sea ice anomaly in 2007 a key contributor to severe January 2008 snowstorm in China? *International Journal of Climatology*, 32: 2081–2087. https://doi.org/10.1002/joc.2400

Makhotina, M. S., & Dmitrenkob, I. A. (2011). Interannual Variability of Pacific Summer Waters in the Arctic Ocean. *Doklady Earth Sciences*, 438(3): 730–732. https://doi.org/10.1134/s1028334x11050345

Nishino, S., Kikuchi, T., Fujiwara, A., Hirawake, T., & Aoyama, M. (2016). Water mass characteristics and their temporal changes in a biological hotspot in the southern Chukchi Sea. *Biogeosciences*, 13, 2563–2578. https://doi.org/10.5194/bg-13-2563-2016

Wang, Y. J., Liu, N., Lin, L. N., He, Y., Kong, B., Zhang, Z. H. (2020). Variation in water masses on shelf of northern Bering Sea in September 2016–2018. *Marine Geodesy*, 43(3): 285–301. https://doi.org/10.1080/01490419.2020.1718256

Weingartner, T., Aagaard, K., Woodgate, R., Danielson, S., Sasaki, Y., & Cavalieri, D. (2005). Circulation on the north central Chukchi Sea shelf. *Deep-Sea Research II*, 52, 3150–3174. https://doi.org/10.1016/j.dsr2.2005.10.015

Woodgate, R. A. (2018). Increases in the Pacific inflow to the Arctic from 1990 to 2015, and insights into seasonal trends and driving mechanisms from year-round Bering Strait mooring data. *Progress in Oceanography*, 160, 124–154. https://doi.org/10.1016/j.pocean.2017.12.007

Woodgate, R. A., & Aagaard, K. (2005). Revising the Bering Strait freshwater flux into the Arctic ocean. *Geophysical Research Letters*, 32, L02602. https://doi.org/10.1029/2004GL021747

Woodgate, R. A., Aagaard, K., & Weingartner, T. J. (2005). A year in the physical oceanography of the Chukchi Sea: Moored measurements from autumn 1990-1991. *Deep-Sea Research II*, 52: 3116–3149. https://doi.org/10.1016/j.dsr2.2005.10.016

Yamashita, Y., Yagi, Y., Ueno, H., Ooki, A., & Hirawake, T. (2019). Characterization of the water masses in the shelf region of the Bering and Chukchi Seas with fluorescent organic matter. *Journal of Geophysical Research: Oceans*, 124: 7545–7556. https://doi.org/10.1029/2019jc015476